Food Chemistry 456 (2024) 140038

Contents lists available at ScienceDirect

Food Chemistry

journal homepage: www.elsevier.com/locate/foodchem

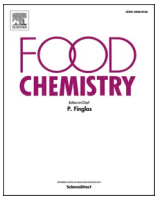

Effect of ohmic heating on the structure and properties of flexible multilayer packaging

Luís Marangoni Júnior [a,b,c,*], Rui M. Rodrigues [c,d], Ricardo N. Pereira [c,d], Pedro Esteves Duarte Augusto [e], Danielle Ito [b], Fábio Gomes Teixeira [b], Marisa Padula [b], António A. Vicente [c,d]

[a] Department of Food Engineering and Technology, Faculty of Food Engineering, University of Campinas (Unicamp), 13083-862, Campinas, SP, Brazil
[b] Packaging Technology Center, Institute of Food Technology, 13073-148, Campinas, São Paulo, Brazil.
[c] CEB – Centre of Biological Engineering, University of Minho, Campus de Gualtar, 4710-057, Braga, Portugal
[d] LABBELS – Associate Laboratory, 4710-057, Braga, Guimarães, Portugal
[e] Université Paris-Saclay, CentraleSupélec, Laboratoire de Génie des Procédés et Matériaux, Centre Européen de Biotechnologie et de Bioéconomie (CEBB), 3 rue des Rouges Terres 51110 Pomacle, France.

ARTICLE INFO

Keywords:
Emerging technology
Food packaging
Tensile strength
Heat sealing strength
Barrier properties
Food thermal process

ABSTRACT

Food-packaging-processing interactions define packaging materials' performance properties and product quality. This study evaluated the effect of ohmic heating (OH) processing and different food simulants on the properties of four multilayer flexible packaging materials (PET_{met}/PE, PET_{met}/PP, PET/Al/PE, and PET/Al/PA/PP). OH treatment was applied to the sealed packages containing the food simulants using a voltage gradient of 3.7 V/cm at a frequency of 20 kHz, resulting in a thermal process of at 80 °C for 1 min. The structure and performance of the different packages were then evaluated. The materials did not show changes in chemical groups nor thermal properties. However, the simulant-packaging-processing interaction resulted in changes in crystallinity, morphology, mechanical and barrier properties (water and oxygen), especially for metallized films in contact with acidic food simulants. The results indicate that although OH resulted in changes in packaging materials, these materials can be used under the conditions applied in this study.

1. Introduction

Industrial processes demand around 1/3 of global energy, generating significant potential to reduce and/or manage energy consumption (Napp et al., 2014; Sakr & Liu, 2014). Particularly in the food industry, energy is necessary to increase the temperature of the process, such as generating steam, hot water, heating food, among others. In such processes, heat can be generated directly or indirectly transferring heat to the material, and be produced from fuels, electric energy and others (Sakr & Liu, 2014). The quality of a product can be determined by the performance of a heating system (Van Der Gotot et al., 2016). However, efficient systems to manufacture products with the required quality and at the lowest cost are necessary.

Thus, the development of new food processes, with the aim of ensuring greater food quality and safety, but also with emphasis on energy efficiency, lower water consumption and reduction of gas and effluent emissions, will reduce food costs production and improve sustainability in the food chain (Fasolin et al., 2019; Misra et al., 2017; Pereira & Vicente, 2010).

Ohmic heating (OH) is a promise technology as it can process food in a short period of time and reduce the energy input (Sakr & Liu, 2014; Yildiz-Turp et al., 2013). Different mechanisms applied during this method reduce the resistance to the heat and mass transfer, compared to conventional methods (Misra et al., 2017; Pereira & Vicente, 2010). OH is defined as a process in which electrical current (usually in alternating mode) passes through conductive materials resulting in internal heat dissipation (Gavahian et al., 2019; Knirsch et al., 2010). The application of the electrical field is made through two electrodes in contact with food, and generally from low to moderate intensity (<1000 V/cm), with a frequency of 50 Hz to 20 kHz (Fasolin et al., 2019). Heating occurs in the form of an internal transformation of energy (from electrical to thermal) within the material, in a very rapid and volumetric heating

* Corresponding author at: Department of Food Engineering and Technology, Faculty of Food Engineering, University of Campinas (Unicamp), 13083-862 Campinas, SP, Brazil.
E-mail address: marangoni.junior@hotmail.com (L. Marangoni Júnior).

https://doi.org/10.1016/j.foodchem.2024.140038
Received 19 April 2024; Received in revised form 23 May 2024; Accepted 7 June 2024
Available online 8 June 2024

(Fasolin et al., 2019; Knirsch et al., 2010), and the amount of heat is directly related to the voltage gradient and electrical conductivity of the product (Yildiz-Turp et al., 2013). However, for processing to occur effectively, the materials must contain sufficient water and electrolytes to allow the passage of electrical current (Knirsch et al., 2010).

This technology is bringing a new paradigm to the thermal processing of foods, reducing excessive thermal load (it does not depend on conduction and convection heat transport mechanisms) and benefiting from the non-thermal effects of electric fields (Fasolin et al., 2019). In addition to rapid heating rates, OH is versatile, allowing to process of various food systems, whether particulate or not, which can lead to increased quality of the final product and increasing its added value. OH has numerous applications, including blanching, evaporation, dehydration, fermentation, extraction, sterilization and heating of foods (Makroo et al., 2020).

To minimize the risk of post-process contamination and avoid expensive aseptic packaging lines, packaging before OH treatment can be considered. Developments for processing OH packaged foods are focused on packaging materials with incorporated aluminum electrodes and conductive packaging materials (Kamonpatana, 2018), with main focus on the food itself (and not the packaging performance). A V-shaped PET/Al/PE (PET: polyethylene terephthalate, Al: aluminum foil and PE: polyethylene) packaging with two metal sheets used as electrodes to heat food was developed, however, heating was not uniform inside the packaging. To facilitate uniform heating, the V-shaped packaging has been redesigned to a rectangular shape with flat sides. A temperature distribution study on a 227 g package showed the presence of cold regions on the electrodeless sides due to current channeling through a hotter, more conductive center (Somavat et al., 2012). A uniform temperature distribution was obtained with the use of two heating strips installed on the external side of the materials (Jun & Sastry, 2005, 2007) Using this approach, treatments at 121 °C for 6 min and 130 °C for 1 min was adequate to inactivate 5 log *Geobacillus stearothermophilus* spores, confirming that sterilization was achieved (Somavat et al., 2012).

On another study, carbon black was incorporated into polypropylene (PP) film due to its conductive properties. The conductive film was connected to the PP film on the left and right sides of the bag to form a rectangular shaped conductive package, liable to be subjected to OH. However, to eliminate the cold zone at the edges and corners of the package, the system required the use of a means to carry the current and channel the electrode current through the package, where the electrical conductivity of the medium was greater than that of the food inside the packaging (Kanogchaipramot et al., 2016). Subsequently, this conductive packaging was used to evaluate the effect of OH in the processing of packaged orange juice. The temperature in the center of the conductive package containing orange juice was 84 °C when a voltage of 300 V was applied for 300 s. A 6 log inactivation of *Escherichia coli* was achieved, indicating that pasteurization of fruit juice using OH through conductive packaging was effective.

Few studies are available in the literature regarding *in-situ* application of OH. In terms of packaging, studies are focused on evaluating the materials' electrical conductivity and heat distribution. To the best of our knowledge, no studies have been carried out that evaluated the effect of OH on the structure and properties of packaging materials, as this technology has great potential for pasteurization and/or sterilization of foods. Still in this context, evaluating the effect of OH on the properties of packaging materials will result in a diagnosis for the application of this technology to process packaged foods. Therefore, the objective of this research was to evaluate the effect of OH processing on the structure and properties of different real packaging materials in the pasteurization range. The innovation lies in the description and understanding of the mechanism of food-packaging-process interaction of this promising emerging technology, paving the application of this technology in the food industry. Finally, for this research, commercial packaging materials widely used for thermo-processed foods and beverages were selected to understand whether these materials are resistant to OH processing.

2. Materials and methods

2.1. Materials

Four multilayer packaging materials (Finepack, São Paulo, Brazil) that are commonly used to package thermo-processed foods were evaluated, as described below:

- PET_{met}/PE (11/44 μm)
- PET_{met}/PP (12/39 μm)
- PET/Al/PE (12/7/45 μm)
- PET/Al/PA/PP (12/7/15/38 μm)

In which PET: polyethylene terephthalate, met: metallized, PE: polyethylene, PP: polypropylene, Al: aluminum foil and PA: polyamide.

2.2. Packaging sample preparation, model foods and ohmic heating processing

The different samples with dimensions of 80 mm × 220 mm were filled with 120 mL of two different food simulants / model foods. The rectangular shape of the packaging materials was selected based on the best distribution of electrical potential and, consequently, the uniformity of heating, as described in the literature (Somavat et al., 2012).

The two evaluated food simulants were: 3% (*v*/v) acetic acid solution and 0.1% sodium chloride solution (*w*/*v*), referred to as AA and NaCl, respectively. Thus, food simulants representing acidic and low-acid food products were considered. The food simulants AA and NaCl showed electrical conductivity of 1597 ± 5 μs cm^{-1} and 1613 ± 45 μs cm^{-1} at 23 °C, respectively.

The OH was performed using two stainless steel electrodes placed on the lateral ends of the inner part of each package. Each package was then hermetically sealed, allowing the external part of the electrodes to be connected to the power system. Through this apparatus, it was possible to apply the OH effect inside the packaging. The supplied voltage, and consequently the temperature, were controlled through the use of a function generator (1 Hz–25 MHz and 1–10 V; Agilent 33220 A, Penang, Malaysia) connected to an amplifier system (4505 Precision Power Amplifier; Miko-Kings Instruments Ltd., Hong Kong, China). The applied electrical frequency was 20 kHz and an electric field intensity of *ca.* 3.7 V/cm was applied until reaching the target treatment temperature of 80 °C. The temperature was measured with a type K thermocouple, placed inside the packaging, in the geometric center of the sample volume. Upon reaching the target treatment temperature, the samples were maintained at 80 °C for 1 min - conditions similar to those applied to pasteurize carrot and apple juices (Abedelmaksoud et al., 2018; Mannozzi et al., 2018, 2019).

For each packaging sample and each food simulant, 10 treatments were carried out. The treatments performed were described as follows: Control (non-processed samples), OH-AA and OH-NaCl. The different samples were characterized in terms of morphology, structure, thermal, mechanical and barrier properties, according to the methods described below.

2.3. Characterization of packaging materials

2.3.1. Fourier-transform infrared (FT-IR) spectroscopy

FT-IR analyzes was performed on a Fourier transform infrared spectrometer (Bruker, Alpha II, Billerica, USA) equipped with attenuated total reflectance (ATR). For all samples, the inner layers were directly analyzed with a spectral resolution of 4 cm^{-1}, 24 scans in the range 4000–600 cm^{-1} (ASTM-E573–01, 2021; ASTM-E1252–98, 2021). The inner layers were selected based on direct contact with the food simulants and also on the configuration of the electrodes, that is, inside the packaging. Three spectra were recorded at different locations on the film for each sample to estimate the average film inhomogeneous

potential and measurement variability.

2.3.2. Differential Scanning Calorimetry (DSC)

The thermal behavior of the packaging samples was evaluated using a differential scanning calorimeter (DSC 6000, Perkin Elmer, Waltham, USA). About 5 mg were weighed and placed in aluminum containers. The test temperature was from 40 °C to 300 °C at a fixed rate of 10 °C/min and pure nitrogen gas flow of 20 mL/min (ASTM-D3418–21, 2021). The melting temperature (T_m) and enthalpy of melting (ΔH) were estimated based on the DSC thermograms. The results were the average of three replications.

2.3.3. X-ray diffraction (XRD)

X-ray diffraction analyzes were performed on an XRD equipment (Bruker D8, Odelzhausen, Germany) with Cu-Kα radiation ($\lambda = 1.54056$ Å, 40 kV, 40 mA at a scan rate of 0.0333°/s). Measurements were obtained with steps of 0.04° from 10° to 30° (2θ) and an acquisition time of 1.2 s. The samples were cut with dimensions of 4 cm × 3 cm and the reading was taken from the internal layer, that is, the layer in direct contact with the food simulants and also according to the configuration of the applied processing, that is, with the electrodes on the inside of the packaging. The percentage of overall crystallinity of the films was estimated by the ratio between the area under the peaks (crystalline regions) and the total area (crystalline and amorphous regions) through deconvolution of the peaks using the free software Fityk. The areas of the curves were determined by numerical integration.

2.3.4. Scanning electron microscopy (SEM)

Morphological analysis of the film surface was performed in an ultra-high resolution Field Emission Gun Scanning Electron Microscopy (FEG-SEM) (NOVA 200 Nano SEM, FEI Company). Topographic images were obtained with a Secondary electron detector at an acceleration voltage of 10 kV. Before morphological analyses samples were covered with a thin film (5 nm) of Au—Pd (80–20 wt%), in a high-resolution sputter coater (208HR Cressington Company), coupled to a MTM-20 Cressington High Resolution Thickness Controller. SEM images were analyzed at 5000× magnification. Similar to FT-IR and XRD analysis, the inner layer was selected to obtain the SEM images.

2.3.5. Mechanical properties

Tensile strength and seal strength tests were carried out at 23 ± 2 °C and 50 ± 5% RH after conditioning the samples for a period of at least 48 h under the same conditions. Samples measuring 25.4 mm wide were used and tests were carried out in the machine direction (MD) and in the transverse direction (TD) of the material. All tests were performed on a universal testing machine (Instron, 5966-E2, Norwood, USA). Tensile strength was determined using a 100 N load cell with a test speed of 50 mm min^{-1} with an initial distance of 40 mm for the MD and 100 mm for the TD. (ASTM-D882, 2018). The seal strength was determined using a 1 kN load cell at a speed of 300 mm min^{-1} and an initial distance of 10 mm. (ASTM-F88/F88M, 2021). The tests were carried out in five replications.

2.3.6. Barrier properties

2.3.6.1. Water vapor transmission rate. The water vapor transmission rate (WVTR) was determined using a PERMATRAN equipment (3/34 G, MOCON, Minneapolis, USA) with an infrared sensor device. The test was carried out at 38 °C and 90% RH with a permeation area of 5 cm^2. WVTR tests were carried out from the outer layer to the inner layer (ASTM-F1249., 2020).

2.3.6.2. Oxygen transmission rate. The oxygen transmission rate (OTR) was determined using an OXTRAN equipment (2/22H, MOCON, Minneapolis, USA). The outer side of the sample was placed in contact with the permeating gas (100% O_2). The test was carried out at 23 °C dry with a permeation area of 5 cm^2. The reading has been corrected for a permeant gas partial pressure gradient of 1 atm. OTR tests were carried out from the outer layer to the inner layer (ASTM-D3985., 2017).

2.4. Statistical analysis

The results were presented as mean ± standard deviation and statistically evaluated by analysis of variance (ANOVA) and Tukey's test to compare mean values ($p < 0.05$).

3. Results and discussion

3.1. Fourier-transform infrared (FT-IR) spectroscopy

The FT-IR spectra of the inner layers of the four films show some characteristic absorption bands for polyethylene - Fig. 1(a) and (c) - and polypropylene - Fig. 1(b) and (d) - films, which are consistent with those reported in the literature (Alaburdaitė & Krylova, 2023; Wang & Ajji, 2022). Regarding the FT-IR spectra of the PE films, the characteristic peaks were attributed to the asymmetric and symmetric stretching vibrations of CH_2 (2915 and 2849 cm^{-1}), respectively, to the C—C stretching vibration (1646 cm^{-1}), to CH deformation vibrations in CH_2 (1471 cm^{-1}), to bending vibrations in CH_3 (1375 cm^{-1}) and to C—C equilibrium vibrations in CH_2 (717 cm^{-1}) (De Geyter et al., 2008; Kochetov & Christen, 2017; Marangoni Júnior et al., 2023; Turriziani, Vieira, et al., 2023). For PP films, the characteristic peaks are attributed to asymmetric and symmetric stretching vibrations in CH_3 and CH_2 (2951 to 2838 cm^{-1}), asymmetric deformation vibrations of CH_3 or scissor vibrations of CH_2 (1456 to 1376 cm^{-1}), to CH_3 symmetric strain vibrations (1359 cm^{-1}) and numerous small peaks in the range referring to C—C asymmetric stretching, CH_3 asymmetric rocking, C—H vibrations, C—C asymmetric stretching vibrations, and to CH_2 oscillation vibrations (1300 to 700 cm^{-1}) (Alaburdaitė & Krylova, 2023; Morent et al., 2008; Smith, 2021). FT-IR is one of the most common and economical methods for analyzing the chemical structure of materials. Thus, it was used to evaluate whether different food simulants and OH would have any influence on the chemical structure of the polymers that make up the internal layer of the studied packaging materials. No changes were observed in the PE and PP spectra after contact with food simulants and OH in relation to untreated films, suggesting that the applied conditions did not modify the chemical nature of PE and PP.

3.2. Differential Scanning Calorimetry (DSC)

Fig. 2 and Table 1 show the thermal profiles and melting temperatures (*Tm*) of each polymeric material of the multilayer structures, as well as the total enthalpies of melting (ΔH) of the entire multilayer structure before and after contact with the different food simulants followed by OH.

For the PET_{met}/PE and PET/Al/PE samples, three melting peaks were observed, with the 1st peak corresponding to LDPE, the 2nd peak corresponding to LLDPE and the 3rd peak corresponding to PET, with T_m values varying between 110.2 °C and 112.3 °C, 117.1 °C to 117.8 °C and 232.3 °C to 241.1 °C, respectively. These ranges are similar to those reported in the literature for LDPE, LLDPE (Benítez et al., 2013; Marangoni Júnior et al., 2023) and PET (Marangoni Júnior, Alves, et al., 2020; Marangoni Júnior, Bócoli, et al., 2020). For the PET_{met}/PP samples, two melting peaks were observed, where the 1st represents PP and the 2nd represents PET. For the PET/Al/PA/PP samples, 3 melting peaks were found, the 1st referring to PP, the 2nd referring to PA and the 3rd to PET. The PET T_m values were close to those described for the PET_{met}/PE and PET/Al/PE samples. Regarding the T_m of PP and PA, the values were 153.1 °C to 155.4 °C and 207.2 °C to 214.5 °C, respectively. Values close to those reported in the literature for PP (Sanetuntikul et al., 2023) and PA (Marangoni Júnior, Dantas, et al., 2020). For the four different

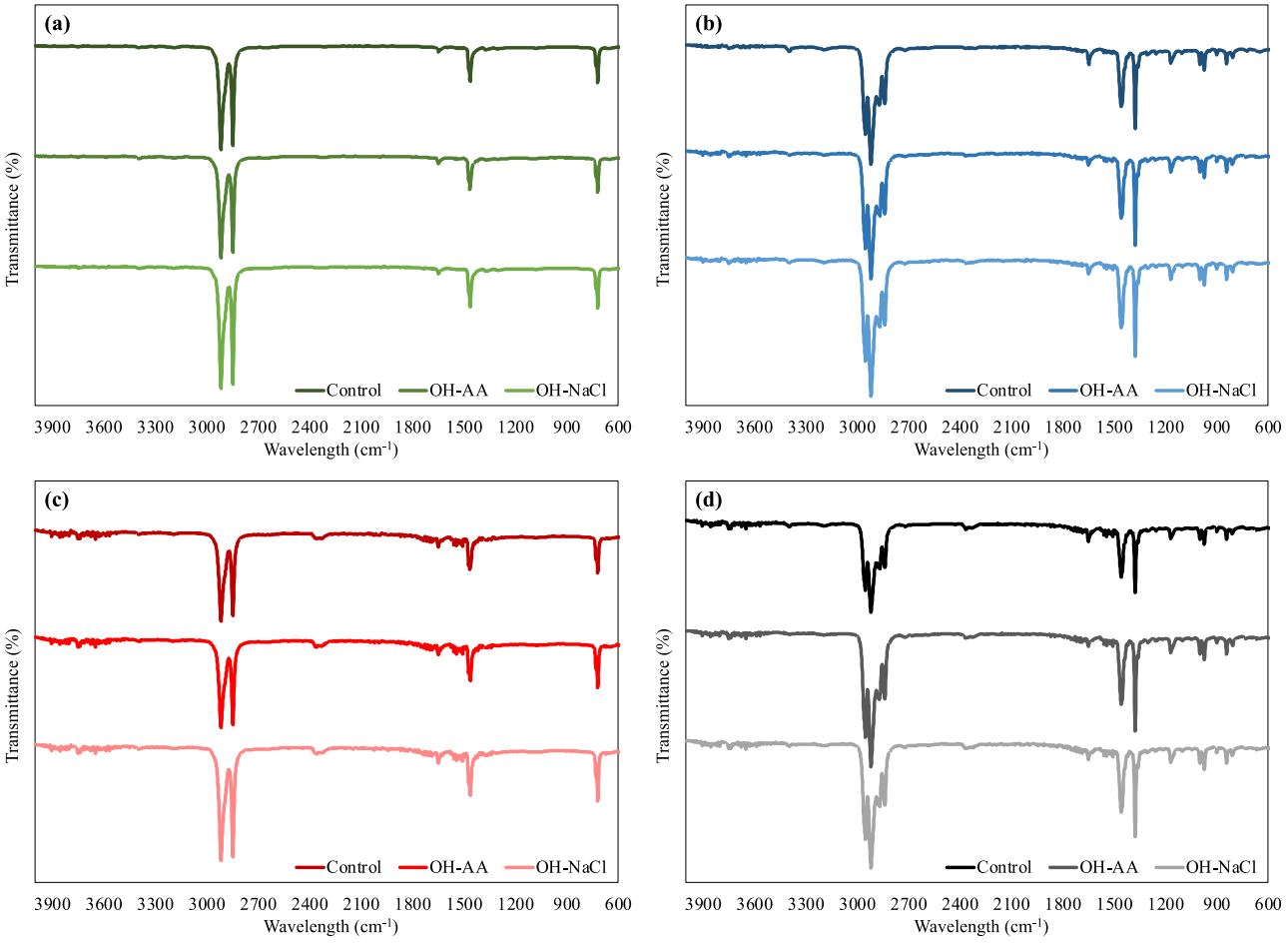

Fig. 1. FT-IR spectra of inner layer of different packaging materials processed by ohmic heating. (a): PET_{met}/PE, (b): PET_{met}/PP, (c): PET/Al/PE and (d): PET/Al/PA/PP.

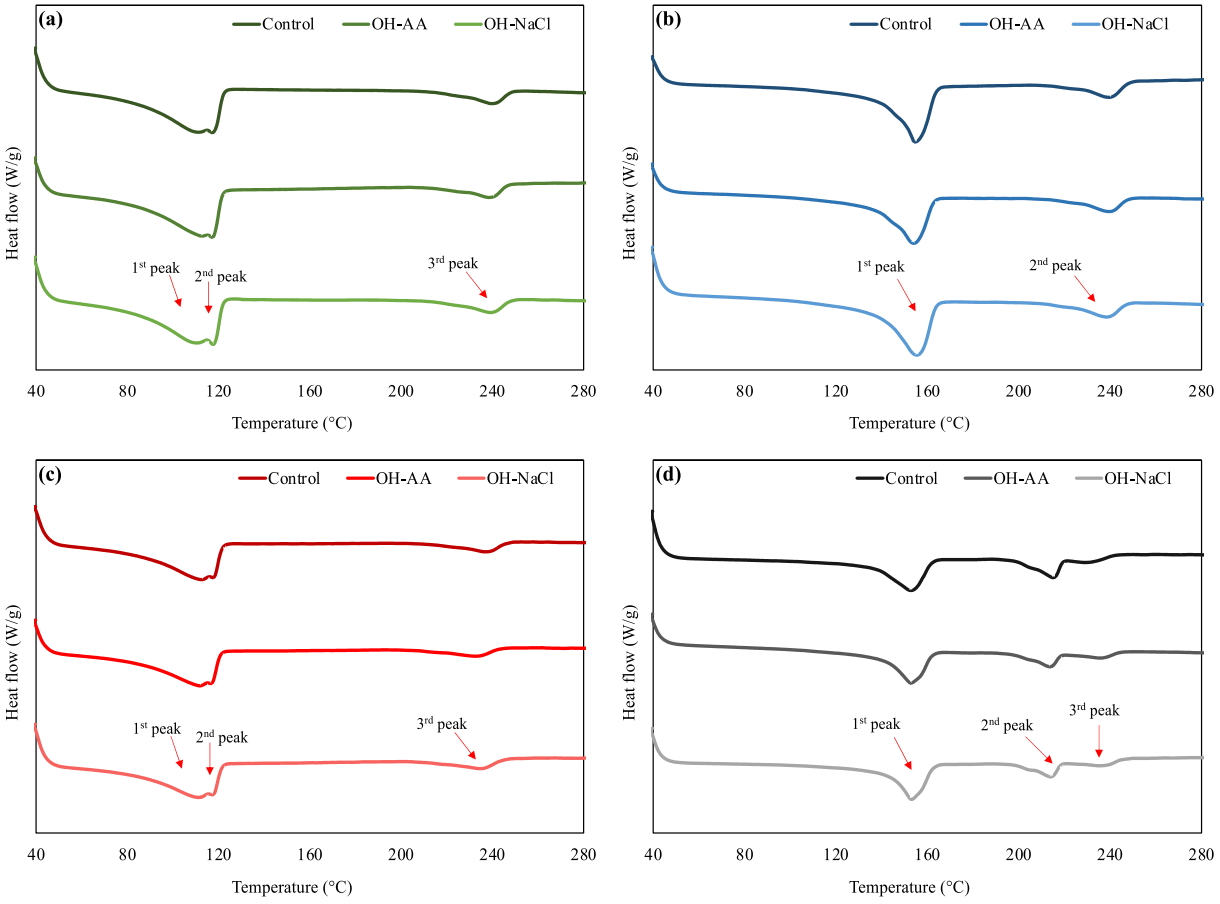

Fig. 2. DSC of different packaging materials processed by ohmic heating. (a): PET_{met}/PE, (b): PET_{met}/PP, (c): PET/Al/PE and (d): PET/Al/PA/PP.

Table 1
DSC results of different flexible packaging materials processed by ohmic heating.

Packaging material	Thermal property	Processing condition		
		Control	OH-AA	OH-NaCl
PET_{met}/PE	T_m (°C) 1st peak	110.2 ± 2.5 [a]	111.2 ± 2.2 [a]	110.2 ± 1.1 [a]
	T_m (°C) 2nd peak	117.8 ± 0.5 [a]	117.2 ± 0.3 [a]	117.8 ± 0.2 [a]
	T_m (°C) 3rd peak	240.0 ± 0.6 [a]	241.1 ± 3.2 [a]	240.1 ± 1.9 [a]
	ΔH^* (J/g)	83.9 ± 12.7 [a]	80.1 ± 16.2 [a]	87.4 ± 16.3 [a]
PET_{met}/PP	T_m (°C) 1st peak	154.9 ± 0.4 [a]	155.1 ± 0.7 [a]	155.4 ± 0.1 [a]
	T_m (°C) 2nd peak	240.7 ± 1.7 [a]	242.5 ± 2.8 [a]	239.6 ± 0.8 [a]
	ΔH^* (J/g)	84.7 ± 3.2 [a]	73.8 ± 5.5 [a]	73.7 ± 11.2 [a]
PET/Al/PE	T_m (°C) 1st peak	110.9 ± 2.0 [a]	112.3 ± 0.4 [a]	110.6 ± 2.0 [a]
	T_m (°C) 2nd peak	117.8 ± 0.3 [a]	117.2 ± 0.5 [a]	117.1 ± 0.4 [a]
	T_m (°C) 3rd peak	232.3 ± 8.1 [a]	233.2 ± 0.3 [a]	232.9 ± 2.6 [a]
	ΔH^* (J/g)	60.0 ± 14.4 [a]	59.7 ± 12.5 [a]	58.0 ± 14.2 [a]
PET/Al/PA/PP	T_m (°C) 1st peak	153.7 ± 0.9 [a]	153.1 ± 0.6 [a]	153.2 ± 0.1 [a]
	T_m (°C) 2nd peak	207.2 ± 11.4 [a]	207.9 ± 10.6 [a]	214.5 ± 0.6 [a]
	T_m (°C) 3rd peak	232.3 ± 0.7 [a]	234.4 ± 3.1 [a]	236.9 ± 0.6 [a]
	ΔH^* (J/g)	45.3 ± 6.0 [a]	42.9 ± 6.3 [a]	44.7 ± 6.2 [a]

T_m: melting temperature and ΔH^*: total enthalpy of melting.
Values referring to the mean of three repetitions ± standard deviation.
[a,b,c] means followed by the same letter in the line do not differ at the 95% confidence level ($p < 0.05$).

multilayer packaging materials, T_m and ΔH were not significantly influenced by the food simulant in contact with the material and by OH, showing that the materials are thermally stable for the conditions in which they were subjected.

3.3. X-ray diffraction (XRD)

The X-ray diffraction patterns of the different samples before and after OH are shown in Fig. 3. For the metallized films (PET_{met}/PE and PET_{met}/PP) a crystalline peak is observed at the angular position of $2\theta = 26°$ - Figs. 3 (a) and (b). These peaks are attributed to the semi-crystalline structure of PET (Dasdemir et al., 2012). The peaks at approximately $2\theta = 21°$ correspond to PE (Fig. 3(a)) (Turriziani, Perez, et al., 2023) and the less intense peaks between $2\theta = 15°$ and 21° correspond to PP (Fig. 3(b)) (Yetgin, 2019). For the PET/Al/PE sample, the PE crystalline peak is also observed at approximately $2\theta = 21°$ (Fig. 3 (c)) and for the PET/Al/PA/PP sample in addition to the PP peak at $2\theta = 15°$ a more intense peak is observed at approximately $2\theta = 24°$ referring to PA (Fig. 3(d)) (Bhunia et al., 2016; Marangoni Júnior et al., 2023).

The overall crystallinity of PET_{met}/PE films processed by OH was higher compared to the control, suggesting that OH induced crystallization of this material. This increase can be attributed mainly to PET, as it is susceptible to the phenomenon of chemicrystallization, where hydrolytic degradation of the polymer occurs at temperatures above the glass transition of PET (65–75 °C). During this process, the amorphous region undergoes chain scission to produce smaller chain fragments with greater mobility, which aids in crystallization (Bhunia et al., 2016; Sammon et al., 2000). On the other hand, the overall crystallinity of the PET_{met}/PP films was lower after OH, where possibly high temperature processing led to a fragmentation of the crystalline structure that was ordered differently upon cooling. Similar behavior was also observed for multilayer films with PP layer processed by conventional heating and microwave-assisted thermal sterilization (Bhunia et al., 2016; Dhawan et al., 2014). The same behavior was observed for PET/Al/PA/PP films, which may also be the result of exposure of the film's hydrophilic polymer (PA) in an environment with high humidity, resulting in the plasticization of the PA and consequently causing some distortions in the crystalline structure of the polymer (Miri et al., 2009; Parodi et al., 2017). Finally, in PET/Al/PE samples almost no change in crystallinity was observed after OH, with values varying between 20.6% and 21.6%. In this sense, the main hypothesis is that changes must also have occurred in the crystalline rearrangement of this material during high-temperature processing. However, after cooling, this rearrangement returned to its initial conformation, thus minimizing the impact on crystallinity.

3.4. Film surface morphology

Scanning electron microscopy was used to visualize the surface morphologies of the films' inner layers before and after OH, as shown in Fig. 4.

The PET_{met}/PE sample showed a rough surface - Figs. 4 (a), (b) and (c) - similar to that found for the PET/Al/PE samples - Figs. 4 (g), (h) and (i). In relation to the PET_{met}/PP and PET/Al/PA/PP samples, the surfaces were more homogeneous and had a smooth appearance - Figs. 4 (d), (e) and (f)) and Figs. 4 (j), (k) and (l) - respectively. This difference between the materials is associated with the polymer of the inner layer being different, where PE has greater roughness compared to PP. It is observed that after OH the PET_{met}/PE sample showed small inclusions that differ from the other samples (Fig. 4(b)) and in the PET_{met}/PP sample some holes were detected (Fig. 4(e)), which is associated with the food simulant-packaging-processing interaction, mainly considering that the acidic food simulant is considered the most critical simulant for metallized packaging. In relation to films laminated with aluminum foil (Al) treated by OH, it is also possible to observe some inclusions and some typical defects related to bending and/or crushing of the aluminum foil, but without breaking the aluminum layer. The defects caused by processing and interaction with food simulants are not perceptible to the human eye. However, as it is necessary to assess whether they cause any damage to the material barrier that makes the use of these packaging in this application unfeasible. This approach is presented in section 3.6.

3.5. Mechanical properties

The tensile strength (TS) and elongation at break (EB) results in the machine direction (MD) and transverse direction (TD) of the different samples before and after OH are presented in Fig. 5. The tests were carried out in two different directions of the material (MD and TD), as in general the mechanical properties are influenced by the orientation of

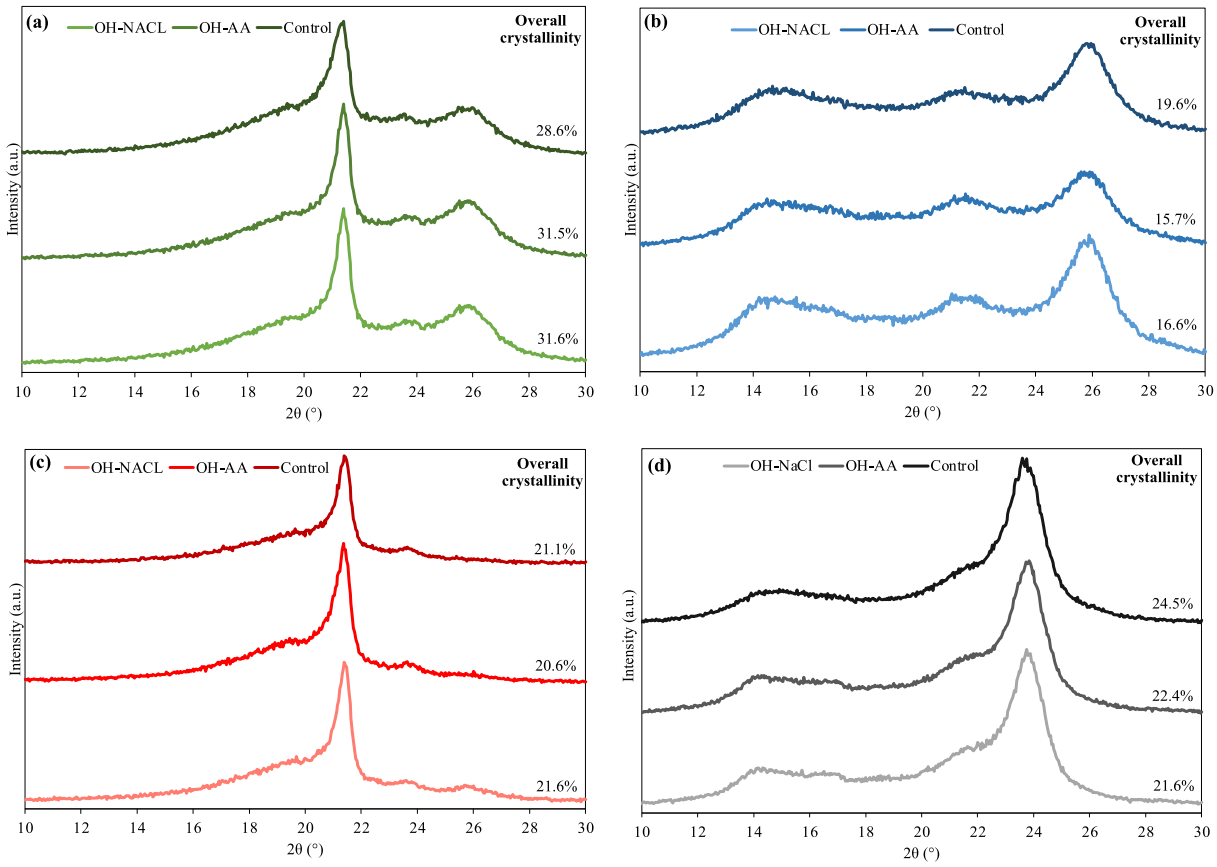

Fig. 3. X-ray diffraction patterns of different packaging materials processed by ohmic heating. (a): PET_{met}/PE, (b): PET_{met}/PP, (c): PET/Al/PE and (d): PET/Al/PA/PP.

the molecules in the manufacture of the film, that is, they differ in relation to the direction of the material. The TS values in the MD and TD showed no significant difference between the processed and unprocessed samples, with the exception of the PET_{met}/PE sample which showed a significant reduction in TS in TD (Fig. 5(a)). Regarding EB, OH did not result in significant changes in both directions of the material when compared to the control, an exception was for the PET/Al/PA/PP film, which showed a significant reduction in EB in TD (Fig. 5 (H)). These small changes in TS and EB may possibly be associated with changes in the degree of crystallinity of the polymers after OH. However, this behavior did not present a trend for all samples and as the changes were punctual and minimal, it can be concluded that OH in the applied conditions did not result in a negative impact on the tensile properties of the materials studied – a positive result.

The multilayer PET_{met}/PE and PET/Al/PE materials presented maximum seal strength values equal to or greater than those of materials composed of PET_{met}/PP and PET/Al/PA/PP, this result is attributed to the excellent characteristics sealing of the PE layer. For metallized films (PET_{met}/PE and PET_{met}/PP) OH did not result in significant changes in seal strength, regardless of the food simulant in contact with the material (Fig. 6(a) and (b)). However, for the PET/Al/PE film, OH resulted in a significant increase in the maximum seal strength in MD (Fig. 6(c)), which may be due to overheating of the film due to of the presence of aluminum foil in the multilayer structure, as highlighted by Kamonpatana (2018) and Kanogchaipramot et al. (2016). Thus, the hypothesis is that this overheating possibly led to an increase in the temperature of the PE film, reaching close to the PE melting temperature (Table 1), favoring the fusion of the sealing layer and consequently resulting in more resistant bonds between the layers interfaces of the sealing layers when cooling the polymer. In principle, this result is not negative. On the other hand, the PET/Al/PA/PP film processed by OH showed a tendency to reduce the maximum seal strength values in MD in relation to the control (Fig. 6(d)), possibly due to the increase in pressure inside the packaging. Furthermore, this reduction may be based on the hypothesis that the presence of a polar polymer (PA) in the structure, which may have favored the absorption of food simulants and consequently had an impact on the sealing layer (Marangoni Júnior et al., 2023). However, no leakage was observed in the packaging sealing region after OH, thus ensuring the integrity of the packaging. It should also be noted that even though there is a reduction in the seal strength of the films, these values are within those recommended for sterilizable bags, as described by (Marangoni Júnior, Dantas, et al., 2020).

3.6. Barrier properties

The WVTR and OTR results of the different films before and after OH are presented in Table 2. The WVTR of the PET_{met}/PE and PET_{met}/PP control metallized films were 1.79 ± 0.23 $g_{water}.m^{-2}.day^{-1}$ and 1.52 ± 0.21 $g_{water}.m^{-2}.day^{-1}$, respectively. Regarding OTR, the values were 5.45 ± 0.46 $mL_{(STP)}.m^{-2}.day^{-1}$ and 5.94 ± 0.67 $mL_{(STP)}.m^{-2}.day^{-1}$, respectively. For PET/Al/PE and PET/Al/PA/PP films, the WVTR and OTR were below the quantification limit of the equipment used. These results are similar to those previously reported for metallized and aluminum foil laminated films (Dantas et al., 2022; Marangoni Júnior et al., 2018; Marangoni Júnior, Alves, et al., 2020). The greater barrier to oxygen and water vapor of films laminated with aluminum foil in relation to metallized films is attributed to the excellent barrier properties of the aluminum foil and the absence of microholes in the Al layer, as observed in Figs. 4 (g) and (j).

It is observed that OH in synergy with the acidic food simulant resulted in a significant increase in the WVTR of the PET_{met}/PE film and the OTR of the PET_{met}/PE and PET_{met}/PP films. These results are

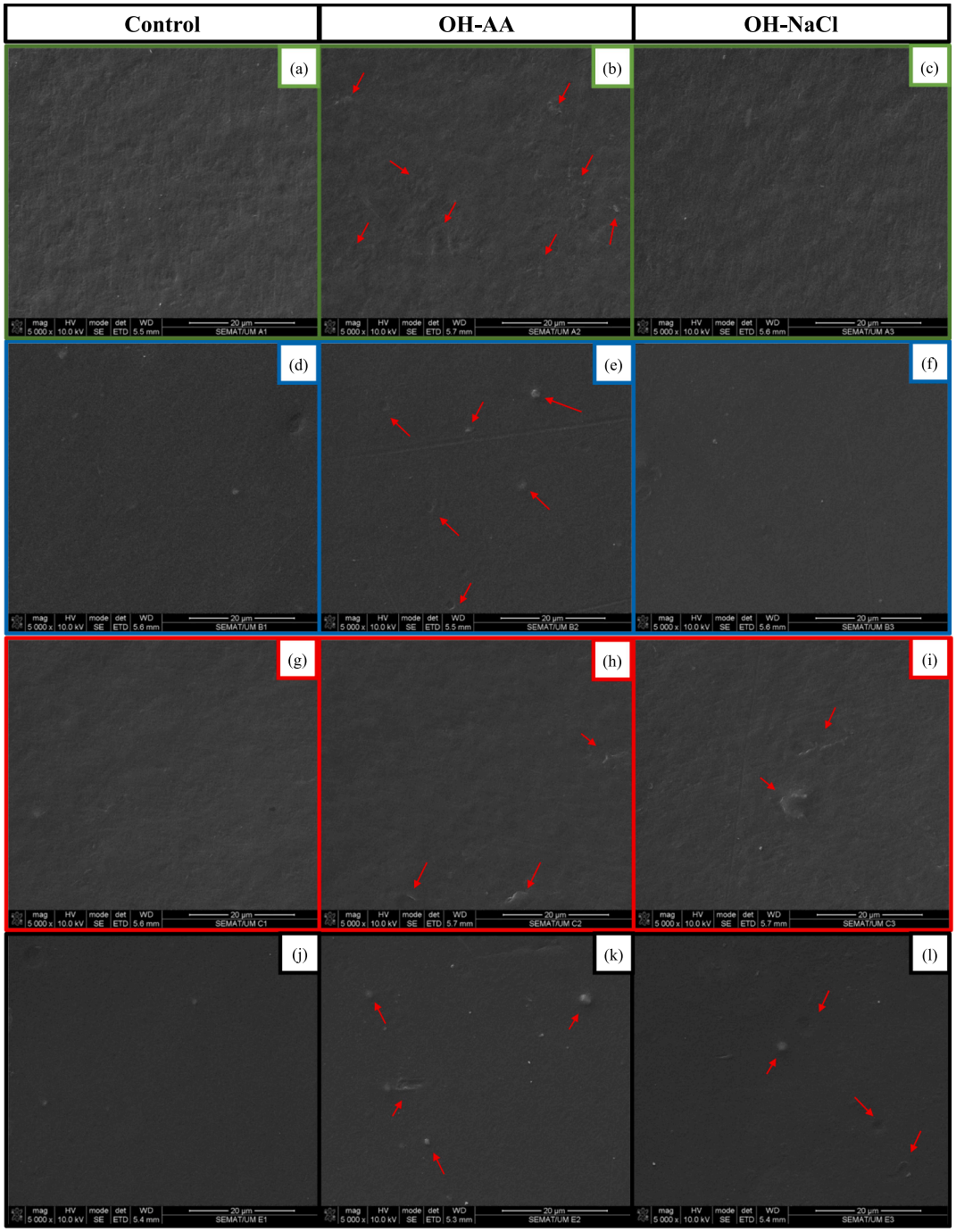

Fig. 4. Scanning electron microscopy of the inner layers surface of different packaging materials processed by ohmic heating. (a, b and c): PET_{met}/PE, (d, e and f): PET_{met}/PP, (g, h and i): PET/Al/PE and (j, k and l): PET/Al/PA/PP. The red arrows indicate changes on the film surface. (For interpretation of the references to colour in this figure legend, the reader is referred to the web version of this article.)

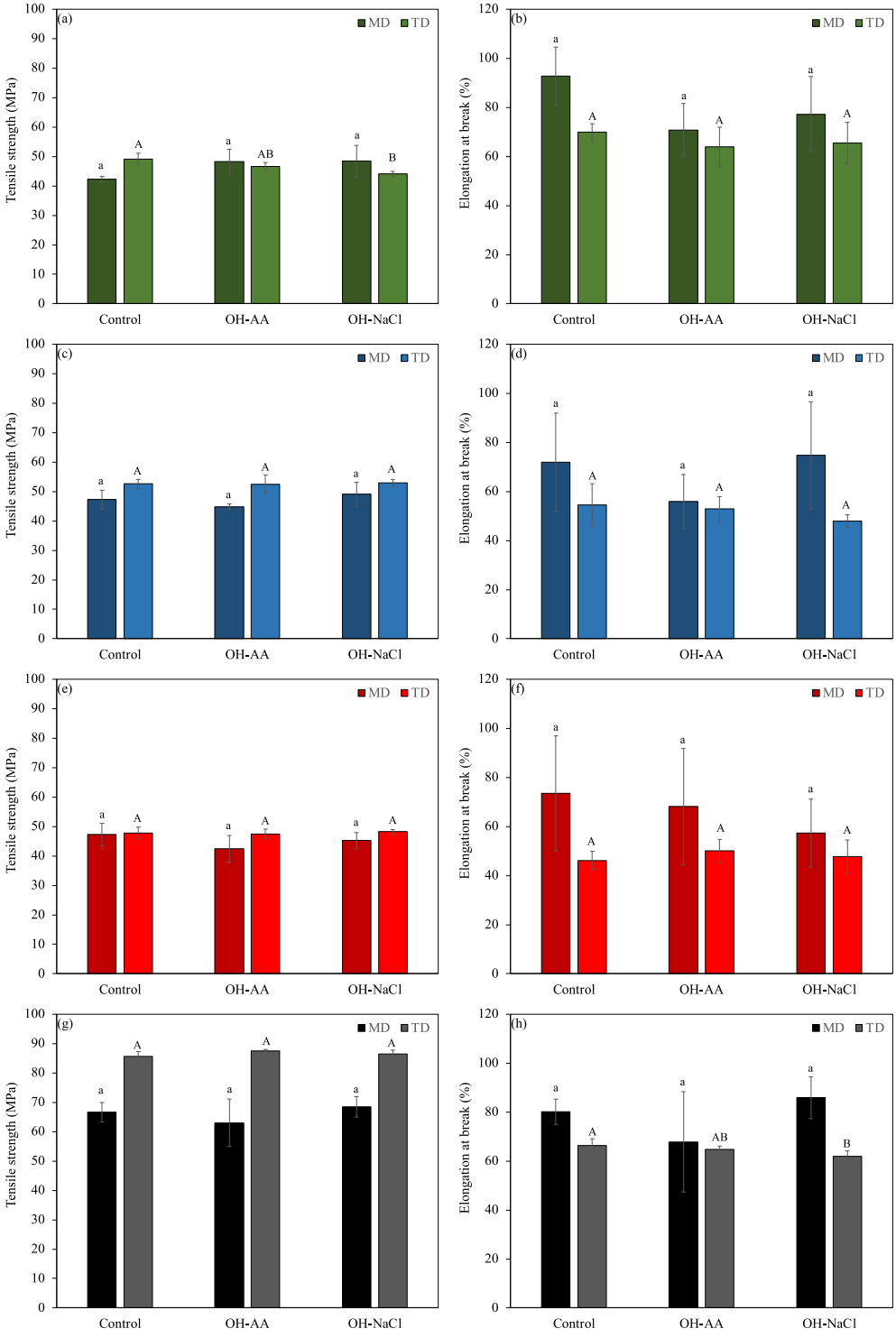

Fig. 5. Tensile strength (a)(c)(e)(g) and elongation at break (b)(d)(f)(h) of different packaging materials processed by ohmic heating. (a)(b): PET_{met}/PE, (c)(d): PET_{met}/PP, (e)(f): PET/Al/PE, (g)(h): PET/Al/PA/PP, MD: machine direction and TD: transverse direction. Lowercase letters (MD) and uppercase letters (TD) do not differ at the 95% confidence level ($p < 0.05$).

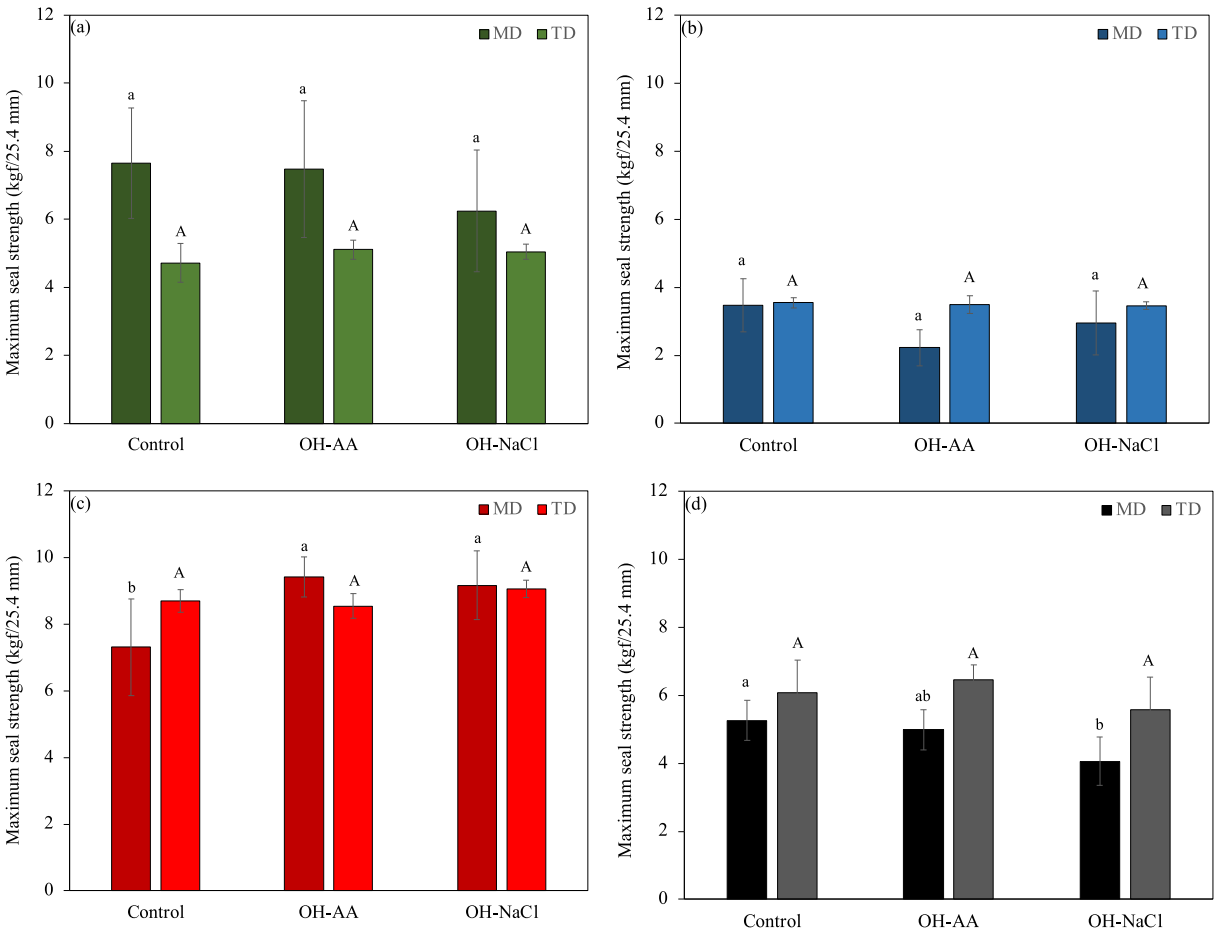

Fig. 6. Maximum seal strength of different packaging materials processed by ohmic heating. (a): PET_{met}/PE, (b): PET_{met}/PP, (c): PET/Al/PE, (d): PET/Al/PA/PP, MD: machine direction and TD: transverse direction. Lowercase letters (MD) and uppercase letters (TD) do not differ at the 95% confidence level ($p < 0.05$).

Table 2
WVTR and OTR of different packaging materials processed by ohmic heating.

Packaging material	WVTR ($g_{water}.m^{-2}.day^{-1}$) 38 °C/90% RH			OTR ($mL_{(STP)}.m^{-2}.day^{-1}$) 23 °C		
	Control	OH-AA	OH-NaCl	Control	OH-AA	OH-NaCl
PET_{met}/PE*	1.79 ± 0.23^{b}	5.22 ± 1.19^{a}	2.77 ± 0.37^{b}	5.45 ± 0.46^{b}	21.28 ± 2.72^{a}	7.46 ± 0.83^{b}
PET_{met}/PP*	1.52 ± 0.21^{a}	3.69 ± 0.93^{a}	3.48 ± 1.25^{a}	5.94 ± 0.67^{b}	9.70 ± 1.88^{a}	5.21 ± 0.49^{b}
PET/Al/PE**	$<0.01^{(1)}$	$<0.01^{(1)}$	$<0.01^{(1)}$	$<0.05^{(1)}$	$<0.05^{(1)}$	$<0.05^{(1)}$
PET/Al/PA/PP**	$<0.01^{(1)}$	$<0.01^{(1)}$	$<0.01^{(1)}$	$<0.05^{(1)}$	$<0.05^{(1)}$	$<0.05^{(1)}$

Values referring to the mean of *three and **two repetitions ± standard deviation.
[1] Results below the quantification limit of equipment.
[a,b,c] means followed by the same letter in the line do not differ at the 95% confidence level ($p < 0.05$).

attributed to the defects observed in the SEM images (Fig. 4) and may also have some association with changes in the overall crystallinity of the films. It should be noted that the acidic food simulant is the most critical simulant in terms of interaction with metallized packaging materials. Added to this, the high process temperature (80 °C) possibly favored interactions between the food simulant and the packaging material, which consequently had an impact on the film barrier. However, this behavior does not prevent the use of the material for this application, if an assessment is made regarding the impact that this loss of barrier will have on the stability of acidic foods treated by OH during storage. This is to ensure that the materials do not compromise the product's quality. In relation to PET/Al/PE and PET/Al/PA/PP films, OH and the different simulants did not influence the barrier of the materials, which although presented morphological defects, there was no rupture of the aluminum foil, which guaranteed maintenance excellent barrier properties.

4. Conclusions and future research outlook

The different multilayer packaging materials were processed by OH at pasteurization conditions in contact with different food simulants. The materials proved to be stable in terms of chemical structure and thermal properties. On the other hand, the OH associated with different food simulants resulted in an increase in the overall crystallinity of the PET_{met}/PE film and a reduction in the crystallinity of the PET_{met}/PP and PET/Al/PA/PP films. Added to this, OH resulted in changes in the

surface of the films, especially in metallized films in contact with the acidic food simulant. Regarding mechanical properties, OH resulted in a small and punctual reduction in the tensile strength of the PET_{met}/PE film and in the elongation at break of the PET/Al/PA/PP film. Furthermore, there was an increase in the heat-sealing tensile strength of the PET/Al/PE film after OH treatment and a reduction for the PET/Al/PA/PP film. The metallized films in contact with the acidic food simulant followed by OH treatment have an increase in water vapor permeability rate and oxygen permeability rate. Finally, although interactions among food, packaging, and processing have caused modifications to the packaging materials under study, they remain suitable for this application.

Future studies are suggested covering different OH processing conditions, examining other packaging materials and evaluating the impact of post-packaging OH on the quality of different food products, aiming to expand knowledge about food-packaging-processing relationships.

CRediT authorship contribution statement

Luís Marangoni Júnior: Writing – original draft, Validation, Resources, Methodology, Investigation, Funding acquisition, Formal analysis, Data curation, Conceptualization. **Rui M. Rodrigues:** Writing – review & editing, Validation, Methodology, Formal analysis, Conceptualization. **Ricardo N. Pereira:** Writing – review & editing, Validation, Methodology, Formal analysis, Conceptualization. **Pedro Esteves Duarte Augusto:** Writing – review & editing, Formal analysis. **Danielle Ito:** Writing – review & editing, Methodology, Investigation. **Fábio Gomes Teixeira:** Writing – review & editing, Methodology, Investigation. **Marisa Padula:** Writing – review & editing, Validation, Supervision, Resources, Funding acquisition, Conceptualization. **António A. Vicente:** Writing – review & editing, Validation, Supervision, Resources, Funding acquisition, Conceptualization.

Declaration of competing interest

The authors declare that they have no known competing financial interests or personal relationships that could have appeared to influence the work reported in this paper.

Data availability

Data will be made available on request.

Acknowledgments

The authors acknowledge São Paulo Research Foundation (FAPESP) for the post-doctoral fellowship of L. Marangoni Júnior grant #2022/09587-3 and grant #2021/04043-2, Multi-user Equipment Program grant #2018/15758-0 and grant #2018/15759-6, and State Research Institutes Modernization Program grant #2017/50349-0. Ricardo N. Pereira acknowledges FCT for its Assistant Research program under the scope of Scientific Stimulus Employment with reference CEECIND/02903/2017/CP1458/CT0006 (https://doi.org/10.54499/CEECIND/02903/2017/CP1458/CT0006). Communauté urbaine du Grand Reims, Département de la Marne, Région Grand Est and European Union (FEDER Champagne-Ardenne 2014-2020, FEDER Grand Est 2021-2027) are acknowledged for their financial support to the Chair of Biotechnology of CentraleSupélec and the Centre Européen de Biotechnologie et de Bioéconomie (CEBB).

References

Abedelmaksoud, T. G., Mohsen, S. M., Duedahl-Olesen, L., Elnikeety, M. M., & Feyissa, A. H. (2018). Optimization of ohmic heating parameters for polyphenoloxidase inactivation in not-from-concentrate elstar apple juice using RSM. *Journal of Food Science and Technology, 55*(7), 2420–2428. https://doi.org/10.1007/s13197-018-3159-1

Alaburdaitė, R., & Krylova, V. (2023). Polypropylene film surface modification for improving its hydrophilicity for innovative applications. *Polymer Degradation and Stability, 211*, Article 110334. https://doi.org/10.1016/j.polymdegradstab.2023.110334

ASTM-D3418–21. (2021). *Standard test method for transition temperatures and enthalpies of fusion and crystallization of polymers by differential scanning calorimetry (p. 8). West Conshohocken*.

ASTM-D3985. (2017). *Standard test method for oxygen gas transmission rate through plastic film and sheetng using a coulometric sensor (p. 7). West Conshohocken*.

ASTM-D882. (2018). *Standard Test Method for Tensile Properties of Thin Plastic Sheeting. West Conshohocken* (p. 12).

ASTM-E1252–98. (2021). *Standard practice for general techniques for obtaining infrared spectra for qualitative analysis (p. 13). West Conshohocken*.

ASTM-E573–01. (2021). *Standard practices for internal reflection spectroscopy (p. 17). West Conshohocken*.

ASTM-F1249. (2020). *ASTM INTERNATIONAL: Standard test method for water vapor transmission rate through plastic film and sheeting using a modulated infrared sensor (p. 7). West Conshohocken*.

ASTM-F88/F88M. (2021). *ASTM INTERNATIONAL: Standard test method for seal strenth fo flexible barrier materials (p. 11). West Conshohocken*.

Benítez, A., Sánchez, J. J., Arnal, M. L., Müller, A. J., Rodríguez, O., & Morales, G. (2013). Abiotic degradation of LDPE and LLDPE formulated with a pro-oxidant additive. *Polymer Degradation and Stability, 98*(2), 490–501. https://doi.org/10.1016/j.polymdegradstab. 2012.12.011

Bhunia, K., Zhang, H., Liu, F., Rasco, B., Tang, J., & Sablani, S. S. (2016). Morphological changes in multilayer polymeric films induced after microwave-assisted pasteurization. *Innovative Food Science & Emerging Technologies, 38*, 124–130. https://doi.org/10.1016/j.ifset.2016.09.024

Dantas, F. B. H., Alvim, I. D., Miguel, A. M. R. D., & O., Alves, R. M. V., & Marangoni Júnior, L.. (2022). Influence of different packaging materials on the stability of Omega-3-enriched Milk powder during storage. *Journal of Packaging Technology and Research, 6*(3), 225–233. https://doi.org/10.1007/s41783-022-00143-6

Dasdemir, M., Maze, B., Anantharamaiah, N., & Pourdeyhimi, B. (2012). Influence of polymer type, composition, and interface on the structural and mechanical properties of core/sheath type bicomponent nonwoven fibers. *Journal of Materials Science, 47*(16), 5955–5969. https://doi.org/10.1007/s10853-012-6499-7

De Geyter, N., Morent, R., & Leys, C. (2008). Surface characterization of plasma-modified polyethylene by contact angle experiments and ATR-FTIR spectroscopy. *Surface and Interface Analysis, 40*(3–4), 608–611. https://doi.org/10.1002/sia.2611

Dhawan, S., Varney, C., Barbosa-Cánovas, G. V., Tang, J., Selim, F., & Sablani, S. S. (2014). The impact of microwave-assisted thermal sterilization on the morphology, free volume, and gas barrier properties of multilayer polymeric films. *Journal of Applied Polymer Science, 131*(12). https://doi.org/10.1002/app.40376

Fasolin, L. H., Pereira, R. N., Pinheiro, A. C., Martins, J. T., Andrade, C. C. P., Ramos, O. L., & Vicente, A. A. (2019). Emergent food proteins – Towards sustainability, health and innovation. *Food Research International, 125*(April), Article 108586. https://doi.org/10.1016/j.foodres.2019.108586

Gavahian, M., Tiwari, B. K., Chu, Y., Ting, Y., & Farahnaky, A. (2019). Trends in Food Science & Technology Food texture as a ff ected by ohmic heating : Mechanisms involved, recent fi ndings, bene fi ts, and limitations. *Trends in Food Science & Technology, 86*(January), 328–339. https://doi.org/10.1016/j.tifs.2019.02.022

Jun, S., & Sastry, S. (2005). Modeling and optimization of ohmic heating of foods inside a flexible package. *Journal of Food Process Engineering, 28*(4), 417–436. https://doi.org/10.1111/j.1745-4530.2005.00032.x

Jun, S., & Sastry, S. (2007). Reusable pouch development for long term space missions : A 3D ohmic model for verification of sterilization efficacy. *Journal of Food Engineering, 80*, 1199–1205. https://doi.org/10.1016/j.jfoodeng.2006.09.018

Kamonpatana, P. (2018). Packaging for foods processed by Ohmic heating. *In Reference Module in Food Science. Elsevier. Doi.* https://doi.org/10.1016/B978-0-08-100596-5.21411-X

Kanogchaipramot, K., Tongkhao, K., Sajjaanantakul, T., & Kamonpatana, P. (2016). Ohmic heating of an electrically conductive food package. *Journal of Food Science, 81*(12), E2966–E2976. https://doi.org/10.1111/1750-3841.13542

Knirsch, C. M., Santos, C. A., Vicente, A. A. M. D., & O., & Pena, T. C. V.. (2010). Ohmic heating e a review. *Trends in Food Science & Technology, 21*(9), 436–441. https://doi.org/10.1016/j.tifs.2010.06.003

Kochetov, R., Christen, T., & Gullo, F. (2017). FTIR analysis of LDPE and XLPE thin samples pressed between different protective anti-adhesive films. *2017. 1st International conference on electrical materials and power equipment (ICEMPE)*, 49–52. https://doi.org/10.1109/ICEMPE.2017.7982097

Makroo, H. A., Rastogi, N. K., & Srivastava, B. (2020). Ohmic heating assisted inactivation of enzymes and microorganisms in foods: A review. *Trends in Food Science & Technology, 97*, 451–465. https://doi.org/10.1016/j.tifs.2020.01.015

Mannozzi, C., Fauster, T., Haas, K., Tylewicz, U., Romani, S., Dalla Rosa, M., & Jaeger, H. (2018). Role of thermal and electric field effects during the pre-treatment of fruit and vegetable mash by pulsed electric fields (PEF) and ohmic heating (OH). *Innovative Food Science & Emerging Technologies, 48*, 131–137. https://doi.org/10.1016/j.ifset.2018.06.004

Mannozzi, C., Rompoonpol, K., Fauster, T., Tylewicz, U., Romani, S., Dalla Rosa, M., & Jaeger, H. (2019). Influence of pulsed electric field and Ohmic heating pretreatments on enzyme and antioxidant activity of fruit and vegetable juices. *Foods, 8*(7), 247. https://doi.org/10.3390/foods8070247

Marangoni Júnior, L., Alves, R. M. V., Moreira, C. Q., Cristianini, M., Padula, M., & Anjos, C. A. R. (2020). High-pressure processing effects on the barrier properties of flexible packaging materials. *Journal of Food Processing & Preservation*. https://doi.org/10.1111/jfpp.14865

Marangoni Júnior, L., Augusto, P. E. D., Vieira, R. P., Borges, D. F., Ito, D., Teixeira, F. G., … Padula, M. (2023). Food-package-processing relationships in emerging technologies: Ultrasound effects on polyamide multilayer packaging in contact with different food simulants. *Food Research International, 163*, Article 112217. https://doi.org/10.1016/j.foodres.2022.112217

Marangoni Júnior, L., Oliveira, L. M. D., Bócoli, P. F. J., Cristianini, M., Padula, M., & Anjos, C. A. R. (2020). Morphological , thermal and mechanical properties of polyamide and ethylene vinyl alcohol multilayer flexible packaging after high-pressure processing. *Journal of Fodd Engineering, 276*(October 2019). https://doi.org/10.1016/j.jfoodeng.2020.109913

Marangoni Júnior, L., Oliveira, L. M. D., Dantas, F. B. H., Cristianini, M., Padula, M., & Anjos, C. A. R. (2020). Influence of high-pressure processing on morphological, thermal and mechanical properties of retort and metallized flexible packaging. *Journal of Food Engineering, 273*(August 2019). https://doi.org/10.1016/j.jfoodeng.2019.109812

Marangoni Júnior, L., Ito, D., Ribeiro, S. M. L., Silva, M. G. D., & Alves, R. M. V. (2018). Stability of β-carotene rich sweet potato chips packed in different packaging systems. *LWT, 92*. https://doi.org/10.1016/j.lwt.2018.02.066

Miri, V., Persyn, O., Lefebvre, J.-M., & Seguela, R. (2009). Effect of water absorption on the plastic deformation behavior of nylon 6. *European Polymer Journal, 45*(3), 757–762. https://doi.org/10.1016/j.eurpolymj.2008.12.008

Misra, N. N., Koubaa, M., Roohinejad, S., Juliano, P., Alpas, H., Inácio, R. S., … Barba, F. J. (2017). Landmarks in the historical development of twenty fi rst century food processing technologies. *Food Research International, 97*(February), 318–339. https://doi.org/10.1016/j.foodres.2017.05.001

Morent, R., De Geyter, N., Leys, C., Gengembre, L., & Payen, E. (2008). Comparison between XPS- and FTIR-analysis of plasma-treated polypropylene film surfaces. *Surface and Interface Analysis, 40*(3–4), 597–600. https://doi.org/10.1002/sia.2619

Napp, T. A., Gambhir, A., Hills, T. P., Florin, N., & Fennell, P. S. (2014). A review of the technologies, economics and policy instruments for decarbonising energy-intensive manufacturing industries. *Renewable and Sustainable Energy Reviews, 30*, 616–640. https://doi.org/10.1016/j.rser.2013.10.036

Parodi, E., Govaert, L. E., & Peters, G. W. M. (2017). Thermochimica Acta Glass transition temperature versus structure of polyamide 6: A fl ash-DSC study. *Thermochimica Acta, 657*(August), 110–122. https://doi.org/10.1016/j.tca.2017.09.021

Pereira, R. N., & Vicente, A. A. (2010). Environmental impact of novel thermal and non-thermal technologies in food processing. *Food Research International, 43*(7), 1936–1943. https://doi.org/10.1016/j.foodres.2009.09.013

Sakr, M., & Liu, S. (2014). A comprehensive review on applications of ohmic heating (OH). *Renewable and Sustainable Energy Reviews, 39*, 262–269. https://doi.org/10.1016/j.rser.2014.07.061

Sammon, C., Yarwood, J., & Everall, N. (2000). An FT–IR study of the effect of hydrolytic degradation on the structure of thin PET films. *Polymer Degradation and Stability, 67*(1), 149–158. https://doi.org/10.1016/S0141-3910(99)00104-4

Sanetuntikul, J., Ketpang, K., Naknaen, P., Narupai, B., & Petchwattana, N. (2023). A circular economy use of waste metalized plastic film as a reinforcing filler in recycled polypropylene packaging for injection molding applications. *Cleaner Engineering and Technology*. , Article 100683. https://doi.org/10.1016/j.clet.2023.100683

Smith, B. (2021). The infrared spectra of polymers III: Hydrocarbon polymers. *Spectroscopy, 36*(11), 22–25.

Somavat, R., Kamonpatana, P., Mohamed, H. M. H., & Sastry, S. K. (2012). Ohmic sterilization inside a multi-layered laminate pouch for long-duration space missions. *Journal of Food Engineering, 112*(3), 134–143. https://doi.org/10.1016/j.jfoodeng.2012.03.019

Turriziani, B. B., Perez, M.Á. F., Kiyataka, P. H. M., Vieira, R. P., Marangoni Júnior, L., & Alves, R. M. V. (2023). Effect of maleic anhydride-based compatibilizer incorporation on the properties of multilayer packaging films for meat products. *Journal of Polymer Research, 30*(6), 194. https://doi.org/10.1007/s10965-023-03584-y

Turriziani, B. B., Vieira, R. P., Marangoni Júnior, L., & Alves, R. M. V. (2023). Mechanical recycling of multilayer flexible packaging employing maleic anhydride as Compatibilizer. *Journal of Polymers and the Environment*. https://doi.org/10.1007/s10924-023-03057-9

Van Der Gotot, A. J., Pelgrom, P. J. M., Berghout, J. A. M., Geerts, M. E. J., Jankowiak, L., Hardt, N. A., … Boom, R. M. (2016). Concepts for further sustainable production of foods. *Journal of Fodd Engineering, 168*, 42–51. https://doi.org/10.1016/j.jfoodeng.2015.07.010

Wang, C., & Ajji, A. (2022). Ethylene scavenging film based on low-density polyethylene incorporating pumice and potassium permanganate and its application to preserve avocados. *LWT, 172*, Article 114200. https://doi.org/10.1016/j.lwt.2022.114200

Yetgin, S. H. (2019). Effect of multi walled carbon nanotube on mechanical, thermal and rheological properties of polypropylene. *Journal of Materials Research and Technology, 8*(5), 4725–4735. https://doi.org/10.1016/j.jmrt.2019.08.018

Yildiz-Turp, G., Sengun, I. Y., Kendirci, P., & Icier, F. (2013). Effect of ohmic treatment on quality characteristic of meat : A review. *Meat Science, 93*(3), 441–448. https://doi.org/10.1016/j.meatsci.2012.10.013